Karppinen, Anssi; Seisko, Sipi; Lundström, Mari

Atmospheric leaching of Ni, Co, Cu, and Zn from sulfide tailings using various oxidants

Published in:
Minerals Engineering

DOI:
10.1016/j.mineng.2024.108576

Published: 01/02/2024

Document Version
Publisher's PDF, also known as Version of record

Minerals Engineering 207 (2024) 108576

Contents lists available at ScienceDirect

Minerals Engineering

journal homepage: www.elsevier.com/locate/mineng

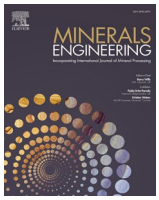

Atmospheric leaching of Ni, Co, Cu, and Zn from sulfide tailings using various oxidants

Anssi Karppinen *, Sipi Seisko, Mari Lundström

Aalto University, School of Chemical Engineering, Department of Chemical and Metallurgical Engineering, P.O. Box 16200, 00076 Aalto, Espoo, Finland

ARTICLE INFO

Keywords:
Pyrite
Pyrrhotite
Sulfuric acid
Ferric ions
Hydrogen peroxide
Oxidative dissolution
Chemical dissolution

ABSTRACT

The growing demand for nickel and cobalt increases the interest in extracting metals from secondary sources, such as flotation tailings. A preferential strategy for the processing of the complex and/or low-grade secondary sources may be material integration into existing primary processes. In this research, a robust sulfuric acid leaching treatment was studied for metal extraction from sulfidic flotation tailings (Ni 0.45 %, Co 0.80 %, Cu 0.20 %, Zn 0.58 %). The impact of leaching parameters on metals extraction was studied; oxygen gas (1–2 L/min), ferric ions (0.05–0.3 M), and hydrogen peroxide (0.5–0.8 M), temperature (30–90 °C), sulfuric acid concentration (0.2–2 M), and solid–liquid ratio (50–100 g/L). It was found that after 30-minutes 20.0 % of nickel, 5.6 % of cobalt, and 33.0 % of the main impurity iron were extracted using oxygen as oxidant. Increasing temperature and sulfuric acid concentration were shown to have a positive effect on extraction. Also, with the further addition of ferric ions, cobalt extraction could be slightly increased (from 6.2 % to 8.3 %) whereas both nickel and cobalt could be increased with hydrogen peroxide (nickel 22.9 %, cobalt 14.2 %). However, the use of H_2O_2 can be challenging due to its high environmental footprint as well as partial decomposition by ferric ions, increasing H_2O_2 consumption further. The results suggest that the mineralogy of the investigated tailings limited feasible metals extraction using atmospheric conditions up to ≈ 20 % for nickel and ≈ 10 % for cobalt, with nickel distributing stronger into non-refractory minerals while cobalt reported more to pyrite. For other base metals, zinc extraction from sphalerite was shown to be efficient (up to ≈ 90 %) whereas copper extraction was limited (up to ≈ 30 %). In future, such atmospheric sulfuric acid leaching may provide a robust recovery route for non-refractory minerals present in the tailings, while full valorization of sulfide tailings matrix will require higher intensity processing with technologies such as pressure oxidation (POX), concentrated chloride leaching, bioleaching, roasting-leaching or very fine milling of the raw material prior to atmospheric leaching.

1. Introduction

The transition towards fossil-free transportation and energy production increases the demand for electrochemical energy storage devices such as lithium-ion batteries (LIBs) (IEA, 2021). Nickel and cobalt are widely used in the cathode active materials of the batteries as well as in other applications such as steel alloys, hard metals, catalysts, and pigments. Based on preliminary estimations by Michaux (2021a; 2021b), global reserves of nickel and cobalt cannot currently meet the forecast demand of these metals as to phase out fossil fuels from vehicles alone, the need of cobalt is larger than estimated reserves and for nickel it is about 50 % of the estimated reserves. According to Savinova et al. (2023), global terrestrial cobalt resources appear to meet forecast cobalt demand until 2040. A wide range of cobalt sources such as deep-sea deposits, mine wastes and tailings are required to meet the future demand (Savinova et al., 2023). Hence, extraction strategies need to be built on alternative raw materials such as lean ores, tailings, slags, and battery waste. In addition to nickel and cobalt, these secondary raw materials often contain other valuable metals such as copper and zinc.

In sulfide tailings, nickel and cobalt are often closely associated with pyrite and pyrrhotite minerals. Nickel and cobalt, along with arsenic and antimony, can be present within the mineral lattice of pyrite up to several percent, thus hindering the selectivity of cobalt and nickel leaching over iron (Abraitis et al., 2004). Two main nickel minerals are pentlandite and nickeliferous pyrrhotite in sulfide ores (Eksteen et al., 2020). Beside pyrite, cobalt can also be present in pentlandite, pyrrhotite, and chalcopyrite (Dehaine et al., 2021). Zinc occurs almost exclusively as sphalerite in sulfides (Nayak et al., 2022).

* Corresponding author.
E-mail address: anssi.karppinen@aalto.fi (A. Karppinen).

https://doi.org/10.1016/j.mineng.2024.108576
Received 1 September 2023; Received in revised form 2 January 2024; Accepted 6 January 2024
Available online 16 January 2024

In acidic solutions, dissolved ferrous iron can be oxidized by oxygen to ferric iron, Reaction 1 (Lu and Dreisinger, 2013). It has been reported that pyrite oxidation is preferred via Fe^{3+} (Reaction 3) rather than by direct gas/solid reaction (Reaction 2) (Descostes et al., 2004; Murphy and Strongin, 2009). Hence, ferrous iron extracted from iron sulfides can be oxidized, and can further catalyze the sulfide minerals leaching reactions (Holmes and Crundwell, 2000). Table 1 shows the possible leaching reactions of the dominant sulfide mineral species (pyrite, pyrrhotite, chalcopyrite, sphalerite, and pentlandite). In general, leaching of sulfides can occur via chemical dissolution by consumption of sulfuric acid or via electrochemical dissolution (oxidative) by dissolved oxygen or ferric ions.

$$4Fe^{2+} + 4H^{+} + O_2 \rightarrow 4Fe^{3+} + 2H_2O \quad (1)$$

Based on the leaching mechanism, sulfide sulfur is converted into elemental form, dissolved sulfate, and/or hydrogen sulfide gas. Chemical dissolution of sulfide minerals at low solution potentials i.e., dissolution of sulfides by consumption of acid can generate toxic hydrogen sulfide gas (Xiao et al., 2020). Hydrogen sulfide may cause in-situ reprecipitation of metals (Arpalahti and Lundström, 2018) or if entering the gas phase and recovered, it can be utilized in further process stages to precipitate nickel, cobalt, and copper intermediate metal sulfide products (Estay et al., 2021). However, under sufficiently oxidative environment, the dissolution of sulfides takes primarily place by oxidation reactions, and formation of hydrogen sulfide can be avoided (Salas-Martell et al., 2020). In atmospheric oxidative leaching processes and medium temperature pressure oxidation (MT-POX) processes below 150 °C, sulfide sulfur is primarily oxidized to elemental sulfur (Jorjani and Ghahreman, 2017). In autoclave processes at high oxygen pressures and temperatures, sulfide sulfur is oxidized to sulfates (Jorjani and Ghahreman, 2017).

Previously investigated leaching methods for Ni-Co sulfide tailings include bioleaching (Ahmadi et al., 2015; Altinkaya et al., 2018; Mäkinen et al., 2021), nitric-sulfuric acid leaching (Xie et al., 2005), and sulfuric acid leaching in pressurized conditions (Magwaneng et al., 2017). Additionally, various pretreatment processes have been proposed such as sulfation roasting (Ozer, 2019), milling (Mäkinen et al., 2021), and flotation (Sirkeci et al., 2006; Magwaneng et al., 2017) to concentrate nickel and cobalt in raw materials and enhance their further extractions. One processing strategy is to conduct leaching in sulfate media to obtain pregnant leach solution (PLS) that can be directly used in state-of-the-art primary nickel and cobalt processing as feed to solution purification and metals recovery processes. Various compositions of industrial Ni-Co solutions are listed Table 2. Ideally, the PLS produced from secondary sources would directly meet the metal concentrations of some of the primary process stages. Iron concentration has to be minimized prior to solvent extraction of Ni and Co (Sole et al., 2005), hence, the secondary solution with high iron concentration needs to be processed by a separate iron removal step. For example, Sahu et al. (2004) have reported that at pH 4.5 iron can be selectively precipitated and concentration decreased from 6.0 to 0.035 g/L while copper, nickel, and cobalt remain dissolved.

The aim of this research is to study a potentially low-cost method i.e., robust atmospheric leaching for sulfide tailings leaching and to extract nickel and cobalt. Additionally, leaching behaviors of other valuable metals—zinc and copper—and the main impurity iron are investigated. In the current study, all the experimental work is carried out in sulfate media to allow pregnant leach solution (PLS) integration into primary nickel and cobalt hydrometallurgical processes. Additionally, the oxidants studied (O_2, Fe^{3+}, H_2O_2) in this research were chosen in such a way that they would not further complicate the PLS purification of the existing processes by introducing atypical impurities. By integration, the capital expenditure needed for standalone purification and recovery processes could potentially be decreased.

Table 1
Possible leaching reactions (Reactions 2–12) of sulfide minerals in sulfuric acid and in the presence of ferric ions at atmospheric pressure.

Mineral	Reaction	Eq.	Ref.
Pyrite	$4FeS_2 + 3O_2 + 12H^{+} \rightarrow 4Fe^{3+} + 8S + 6H_2O$	(2)	Descostes et al., 2004; Braun et al., 1974
	$FeS_2 + 2Fe^{3+} \rightarrow 3Fe^{2+} + 2S$	(3)	
Pyrrhotite	$Fe_7S_8 + 14H^{+} \rightarrow 7Fe^{2+} + 7H_2S + S$	(4)	Mäkinen et al., 2021; Altinkaya et al., 2018
	$2Fe_7S_8 + 28H^{+} + 7O_2 \rightarrow 14Fe^{2+} + 14H_2O + 16S$	(5)	
	$Fe_7S_8 + 14Fe^{3+} \rightarrow 21Fe^{2+} + 8S$	(6)	
Chalcopyrite	$CuFeS_2 + 4H^{+} + O_2 \rightarrow Cu^{2+} + Fe^{2+} + 2S + 2H_2O$	(7)	Hiroyoshi et al., 2002
	$CuFeS_2 + 4Fe^{3+} \rightarrow Cu^{2+} + 5Fe^{2+} + 2S$	(8)	
Sphalerite	$2ZnS + 4H^{+} + O_2 \rightarrow 2Zn^{2+} + 2H_2O + 2S$	(9)	Svens et al., 2003; Mäkinen et al., 2021
	$ZnS + 2Fe^{3+} \rightarrow Zn^{2+} + 2Fe^{2+} + S$	(10)	
Pentlandite	$2Fe_{4.5}Ni_{4.5}S_8 + 9O_2 + 36H^{+} \rightarrow 18H_2O + 9Ni^{2+} + 9Fe^{2+} + 16S$	(11)	Lu et al., 2000
	$2Fe_{4.5}Ni_{4.5}S_8 + 36Fe^{3+} \rightarrow 45Fe^{2+} + 9Ni^{2+} + 16S$	(12)	

2. Materials and methods

2.1. Chemicals

The chemicals used in leaching included sulfuric acid (95 % H_2SO_4, VWR Chemicals), oxygen gas (industrial grade, Woikoski Oy), ferric sulfate pentahydrate (97 % $Fe_2(SO_4)_3{\cdot}5H_2O$, VWR Chemicals), hydrogen peroxide (50 % H_2O_2, Sigma-Aldrich), and ion-exchanged water. Nitric acid (65 % HNO_3, Merck Millipore) was used for liquor sample dilution. Sodium hydroxide (2 M NaOH, Honeywell Fluka), methyl orange indicator (Schering AG, diluted in water with 0.1 wt% concentration), sodium thiosulphate pentahydrate (99.9 % $Na_2S_2O_3{\cdot}5H_2O$, VWR Chemicals) and ion-exchanged water were used for acid-base titration.

2.2. Solution and solid analysis methods

The elemental composition (32 elements) of solids was determined by ALS Finland Oy, using total dissolution followed by Inductive Coupled Plasma Optical Emission Spectrometry (ICP-OES). Leach liquor samples were diluted with 2 % HNO_3 and analyzed by atomic absorption spectrometry (AAS; Thermo Scientific, iCE 3000 series) to determine nickel, cobalt, copper, zinc, and iron concentrations. Additionally, non-diluted leach liquor samples after reduction of Fe(III) to Fe(II) were titrated by NaOH solution to determine acid consumption during the leaching.

Raw material was analyzed using X-ray diffraction (Bruker D8 Discover (A25) powder diffractometer) by GTK, Finland to examine the mineralogical composition. Two XRD measurements were done for the sample: 1) Phase identification for a 150 mg sub-sample and 2) XRD Rietveld work for the sample powder (12 g) that was milled for 20 min and prepared by a side-loading method. X-ray powder diffractograms were measured for 0.5 h for phase identification and 1.5 h for Rietveld refinement with the 2Θ-range 4-110° in continuous measurement mode using X-ray tube settings of 40 kV / 40 mA. Phase identifications were done using Bruker EVA 6.0 software and ICDD (International Center for Diffraction Data). Rietveld refinement was done using PANalytical HighScore Plus 4.9, and the crystal structures of the identified phases were taken from COD (Crystallographic Open Database) or from previously refined and stored structures. Additionally, SEM-EDS (Hitachi, SU3900) analyses were carried out by GTK, Finland. The particle size distribution of solid samples was measured by laser diffraction particle size analyzer (Malvern Panalytical, Mastersizer 3000) using the Fraunhofer scattering model.

Table 2
Metal concentrations in hydrometallurgical nickel and cobalt processes (after iron removal, prior to solvent extraction stages).

Plant	Co	Ni	Zn	Cu	Fe	Notes	Reference
		g/L					
Kasese Cobalt company Ltd, Uganda	3.5	0.2	0.012	0.1	0.04	Feed solution to Zn SX	Sole et al., 2005
Chambishi Metals Plc, Zambia	10.2	0.05	0.001	0.4	0.05	Feed solution to Co SX	Sole et al., 2005
Knightsbridge Cobalt, South Africa	4.8	0.03	0.05	<0.001	<0.001	Feed solution to Co SX	Cole, 2002
Tati Nickel, Botswana	0.2	7.1	–	0.002	–	Feed solution to Co SX	Sole et al., 2005
Nkomati, South Africa	1.9	32.7	0.12	0.01	0.001	Feed solution to Co SX	Feather et al., 2002
Bulong Operations, Australia	0.21	2.8	0.03	0.003	0.002	Feed solution to Co SX	Donegan, 2006
Uranium corporation of India Ltd	0.14	6.0	–	2.47	0.04	Feed solution to Cu SX	Sahu et al., 2004
Caldag Nickel, Turkey	0.24	4.1	–	–	–	Feed solution to Ni SX	Kursunoglu et al., 2017

2.3. Raw material

The raw material was flotation tailings. This sample was composited from different locations of a tailings dam, dried at 60 °C, and homogenized by using a riffle splitter and a rotating sample divider. The main mineral phases of the sulfide tailings were pyrite (FeS_2 = 53.0 wt%), pyrrhotite ($Fe_{(1-x)}S$ = 25.0 wt%), and quartz (SiO_2 = 11.6 wt%). Additionally, minor phases included valuable minerals such as pentlandite ($(Fe,Ni)_9S_8$ = 0.5 wt%) and chalcopyrite ($CuFeS_2$ = 0.3 wt%). Beside quartz, the other gangue minerals in the tailings are actinolite (4.2 wt %), albite-ordered minerals (1.0 wt%), dolomite (1.1 wt%), and below 1 wt% calcite, anthophyllite, talc, biotite, microcline, diopside, hexahydrite, clinochlore, and gypsum.

Nickel (0.45 wt%) is present in pentlandite and possibly also within pyrrhotite and pyrite. The nickel to iron ratio is variable in pentlandite, but typically it contains approximately 36 % Ni and 30 % Fe (Crundwell et al., 2011). Hence, it can be approximated that about 40 % nickel of the raw material is present in pentlandite and the remaining 60 % nickel is present in pyrrhotite and pyrite. For cobalt (0.80 %) no candidate phases were identified, however, cobalt is known to substitute iron in pyrite and minor concentrations can be present in pyrrhotite and pentlandite as well. Other base metals, zinc (0.58 wt%) and copper (0.20 wt%), were also present in the raw material. The main copper containing mineral in the material is chalcopyrite and for zinc the main mineral is sphalerite (ZnS). However, the sphalerite content could not be reliably quantified. The elemental and mineralogical composition of the tailings are listed in Table 3. Fig. 1 shows the particle size distribution of the raw material. Measured d_{10}, d_{50}, and d_{80} values were 10.7 µm, 41.5 µm, and 76.2 µm, respectively. The particle size distribution is in line with reported tailings sizes (Ahmadi et al., 2015; Magwaneng et al., 2017).

2.4. Experimental set-up and leaching series

Leaching experiments were performed in a 1 L glass reactor that is placed in a thermostatic water bath (Aqualine AL 25, Lauda, Germany). Initial lixiviant volume (excluding solids) was 0.7 L in every leaching experiment. The reactor was sealed with a glass cover and silicon corks.

Table 3
Elemental composition and mineralogical composition of the raw material.

Element	Concentration (wt.%)	Mineral	Concentration (wt.%)
Fe	36.3	FeS_2	53.0
S	36.6	$Fe_{(1-x)}S$	25.0
Ni	0.45	$(Fe,Ni)_9S_8$	0.5
Co	0.80	$CuFeS_2$	0.3
Cu	0.20	ZnS	< 1.0
Zn	0.58	SiO_2	11.6
Si	5.70	Others	~ 9
Na	0.058		
K	0.083		
Ca	1.64		
Mg	0.91		
Al	0.31		

The stirring was performed with an overhead stirrer (Vos 16, VWR, Finland) equipped with a four-blade teflon impeller. The oxygen sparge, adjusted by a rotameter, was directed to reactor through a silicon hose and a glass sinter. The sinter head was placed into reactor just above the impeller. All the generated gases were directed to a reflux condenser that was connected to a gas washing bottle containing alkaline wash solution.

Both pH (Multiparameter Meter edge®, Hanna Instruments, USA) and redox potential (Redox Au ORP electrode (Ag/AgCl), Mettler Toledo, Germany) were measured during leaching experiments. The chosen pH and redox electrodes are stable at high temperatures (0–100 °C) and under acidic conditions. Simultaneously with measurements, sampling of 10 mL liquid samples was performed. Measurements and sampling were made at 5, 15, 30, 60, 120, 240, and 360 min. The samples were preserved with 5 M nitric acid. In mild acid ($[H_2SO_4]$ = 0.2 M) leaching experiments, constant acidity was maintained by additions of sulfuric acid at sampling times. After leaching, the pregnant leach solution and the solid residue were separated by vacuum filtration and the filtration cake was washed with ion-exchanged water. The filtration cake was dried at 60 °C for 48 h.

Acid consumption during leaching was determined by acid-base titration using 2 M NaOH solution and methyl orange as an indicator. First, 1 mL leach liquor and 50 mL of ion-exchanged water was measured to an Erlenmeyer flask to fade the color of leach liquor sample. Then, two $Na_2S_2O_3{\cdot}5H_2O$ crystals and five drops of methyl orange were added to the solution to prevent iron precipitation and to indicate neutralization of the solution, and the solution was mixed with magnetic stirring. NaOH was added dropwise from a burette until the color of the solution changed from red to yellow.

Three leaching series were conducted: *LA*, *LB* and *LC*. In the first leaching series (*LA1-15*), the studied parameters were temperature (T = 30–90 °C), *S/L-ratio* (50–100 g/L), sulfuric acid concentration ($[H_2SO_4]$ = 0.2–2.0 M), and oxygen flow (*O_2-flow* = 0–2 L/min). Additionally, repeatability of the method and homogeneity of the sample material was verified by repeating leaching three times (*LA9–11*) using center point conditions (T = 60 °C, *S/L-ratio* = 75 g/L, and $[H_2SO_4]$ = 0.6 M). The following leaching series (*LB1–8*) studied the oxidation effect of initial ferric ion concentration ($[Fe^{3+}]$ = 0.05–0.3 M) with varying sulfuric acid concentration ($[H_2SO_4]$ = 0.5–1.0 M). Ferric ions were dissolved into the lixiviant prior to leaching of tailings. In the third series (*LC1–3*), the effect of hydrogen peroxide (volume of added 25 % H_2O_2 = 40–64 mL) as an oxidant was studied at varying temperatures (T = 30–90 °C). The additions of hydrogen peroxide were made at sampling points (30, 60, 120, and 240 min) to maintain sufficiently high oxidation potential (800 mV (vs. SHE)). At higher temperatures, H_2O_2 consumption was increased so the added volume of 25 % H_2O_2 varied from 40 to 64 mL ($[H_2O_2]$ = 0.5–0.8 M). The parameters that were kept constant in the experimental leaching, were initial volume of lixiviant (0.7 L), agitation speed (350 RPM), and leaching time (360 min). The details of experimental series *LA*, *LB*, and *LC* are listed in Table 4.

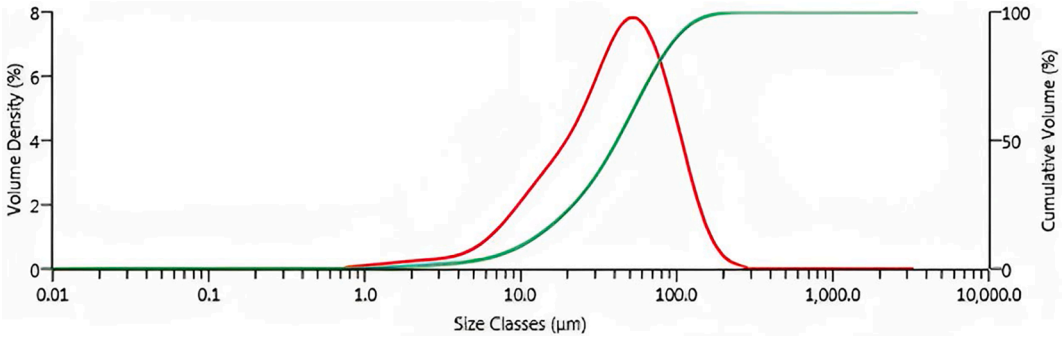

Fig. 1. Particle size distribution of the raw material.

Table 4
Experimental leaching series *LA*, *LB*, and *LC* and their parameters (temperature, solid to liquid-ratio, initial sulfuric acid concentration, oxygen feed, ferric ion concentration, and hydrogen peroxide volume).

Exp. Number	T (°C)	S/L-ratio (g/L)	[H_2SO_4] (M)	O_2 (L/min)	[Fe^{3+}] (M)	25 % H_2O_2 (mL)
LA1	30	50	0.2	2	–	–
LA2	90	50	0.2	2	–	–
LA3	30	100	0.2	2	–	–
LA4	90	100	0.2	2	–	–
LA5	30	50	1	2	–	–
LA6	90	50	1	2	–	–
LA7	30	100	1	2	–	–
LA8	90	100	1	2	–	–
LA9	60	75	0.6	2	–	–
LA10	60	75	0.6	2	–	–
LA11	60	75	0.6	2	–	–
LA12	60	75	0.6	0	–	–
LA13	90	50	2	2	–	–
LA14	60	75	0.6	0	–	–
LA15	60	75	0.6	1	–	–
LB1	90	50	0.5	1	0.05	–
LB2	90	50	1	1	0.05	–
LB3	90	50	0.5	1	0.1	–
LB4	90	50	1	1	0.1	–
LB5	90	50	0.5	1	0.2	–
LB6	90	50	1	1	0.2	–
LB7	90	50	0.5	1	0.3	–
LB8	90	50	1	1	0.3	–
LC1	30	50	1	1	–	40
LC2	60	50	1	1	–	56
LC3	90	50	1	1	–	64

3. Results and discussion

3.1. Leaching in sulfuric acid system (H_2SO_4-O_2)

During the leaching experiments in H_2SO_4-O_2 system (Series *LA*, Table 4), nickel and cobalt extractions were shown to predominantly occur within the first 30 min, Fig. 2. The leaching order and thus nobility (from lowest to highest) of the mineral species has been reported as $Fe_{1-x}S$ – (Zn,Fe)S – $(Fe,Ni)_9S_8$ – $CuFeS_2$ – FeS_2 (Arpalahti and Lundström, 2018). This suggests that dissolved Ni, Co, and Fe originated most likely from pyrrhotite and pentlandite, as chalcopyrite and pyrite do not typically have fast kinetics in sulfuric acid leaching (Sokić et al., 2019; Sun et al., 2015). Copper and zinc extractions were shown to increase as the leaching progressed. However, modestly increasing copper extraction confirmed the refractory nature of chalcopyrite.

The increase in temperature from 30 °C to 90 °C increased cobalt (3.8 % to 6.2 %), nickel (7.1 % to 20.3 %), copper (6.2 % to 23.1 %), and zinc (24.1 % to 83.1 %) extractions, Fig. 2. Additionally, extraction of the main impurity, iron, increased from 5.0 % to 33.0 % i.e., had higher relative extraction at 90 °C when compared to the Ni, Co, and Cu. Based on the quantitative XRD analysis of the raw material, iron is distributed to pyrite, pyrrhotite, pentlandite, and chalcopyrite by proportions of 61.4 %, 38.0 %, 0.4 %, and 0.2 %, respectively. Hence, the extraction of iron (33.0 %) originates mostly from pyrrhotite at 90 °C. It is noteworthy that the highest extraction for iron at 30 min (38.4 %) almost equals the relative iron concentration in pyrrhotite, and during the remaining leaching time, partial reprecipitation of iron occurs.

Based on Fig. 2a (and 4a), it is clear that soluble nickel and cobalt in the tailings were present in different minerals. Although mineralogical analysis suggests Ni and Co being mainly located within pyrite, the leaching behavior shows that ca. 20 % of Ni was present in pyrrhotite and/or pentlandite phases whereas for cobalt only ca. 6 % was soluble and the rest can be assumed to be associated with pyrite.

The final redox potential was lower at 90 °C (605 mV vs. SHE) when compared to the redox potential at 30 °C (680 mV vs. SHE). In addition, acid consumption was higher at 30 °C (192.75 g H_2SO_4 / g Co, Ni, Cu, Zn extracted) when compared to 90 °C (86.4 g H_2SO_4 / g Co, Ni, Cu, Zn extracted), hence, the increase in temperature increased the oxidative dissolution of metals which resulted in the reduced oxidative power of the leaching solution. As the acid consumption was higher at 30 °C, more direct reactions between sulfuric acid and sulfides occurred generating H_2S gas whereas at 90 °C, increased oxidative dissolution resulted in increased oxidation of sulfides to elemental S (Table 1, Reactions 5, 7, 9, and 11). Extensive extraction of iron at 90 °C contributes to further oxidative dissolution of sulfides via ferric ions which results in elemental S formation as well (Table 1, Reactions 6, 8, 10, and 12).

The temperature dependency can be described by the Arrhenius equation (Equation 1).

$$k = Ae^{\frac{-E_a}{RT}} \quad (1)$$

where k is the rate constant ($mol \cdot s^{-1}$), A is a pre-exponential frequency factor ($mol \cdot s^{-1}$), Ea is the activation energy ($J \cdot mol^{-1}$), R is the gas constant (8.314 $J \cdot K^{-1} \cdot mol^{-1}$) and T is the absolute temperature (K) (Laidler, 1984).

For pyrrhotite, the activation energy was determined to be 22.2 kJ/mol (zero order reaction) during the first 60 min of leaching in mild sulfuric acid (0.2 M, Exp. *LA1* and *LA2*) which is similar to reported by Chirita et al. (2002) for pyrrhotite dissolution in hydrochloric acid in the presence of Sn^{2+} (23.3 kJ/mol). In contrast, Janzen et al. (2000) reported 47–63 kJ/mol activation energies for pyrrhotite dissolution by oxygen and ferric ions at pH 2.5. In general, activation energies below 20 kJ/mol are considered diffusion-controlled, between 20 kJ/mol and 40 kJ/mol mixed-controlled, and greater than 40 kJ/mol chemical reaction rate controlled (Faraji et al., 2022). Dissolution of pyrrhotite from the studied raw material is therefore controlled by diffusion rather than chemical reaction. In more concentrated sulfuric acid (1 M), the leaching kinetics of pyrrhotite was considerably faster, but the activation energy was not determined due to complete dissolution of pyrrhotite after 15 min. Passivation of particle surfaces can increase the activation energy, and therefore the effect of mechanical activation by 5-minute

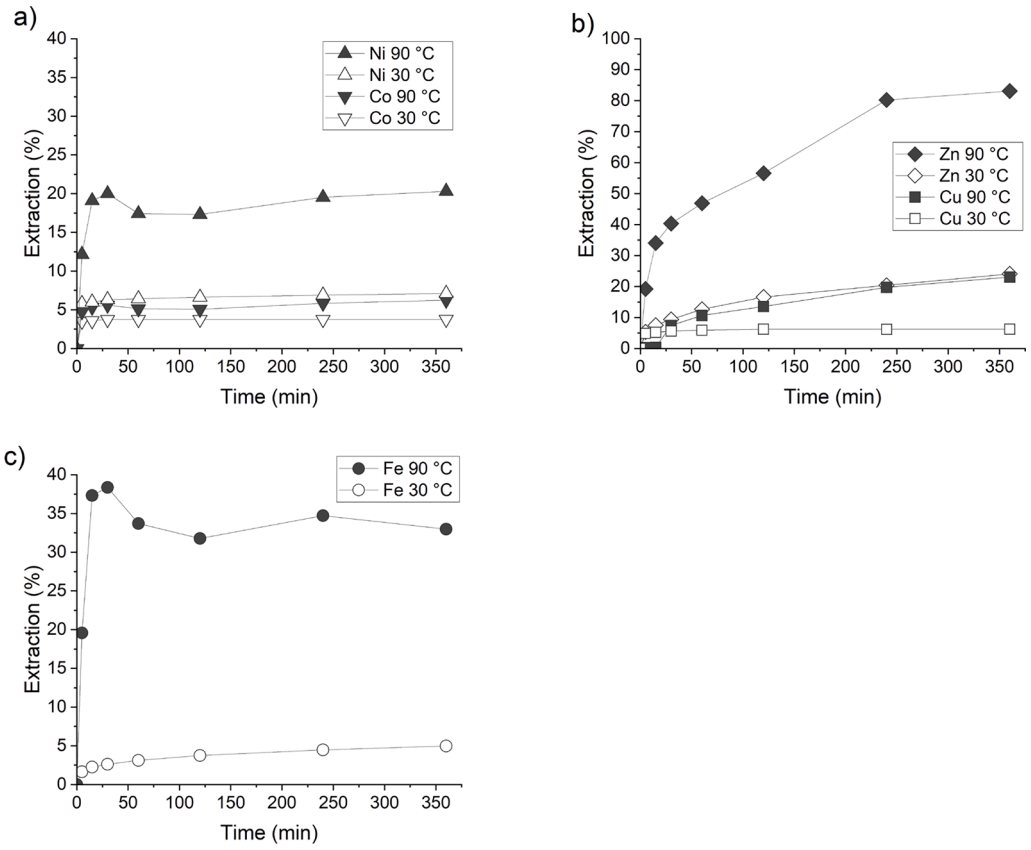

Fig. 2. The effect of temperature on a) cobalt and nickel, b) zinc and copper, and c) iron extraction (Exp. LA5 and LA6: S/L-ratio = 50 g/L; [H_2SO_4] = 1 M; O_2-flow = 2 L/min).

grinding in the ball was studied for the raw material. As the leaching results were almost identical for ground and unground raw material (Fig. 1S), no further mechanical pretreatment was considered.

The impact of temperature on pyrrhotite leaching was positive. Previously, Samadifard et al. (2015) have reported increasing nickel extraction (45–90 %) from pyrrhotite tailings as temperature increased from 30 °C to 55 °C in H_2SO_4-Fe^{3+} leaching. For pyrite leaching, it has been shown that the temperature is a key factor due to high activation energy (>51 kJ/mol) at > 700 mV (vs. SHE) potentials (Sun et al., 2015).

The lower amount of solids (50 g/L) in 1 M sulfuric acid media slightly enhanced cobalt extraction (4.8 % to 6.2 %) and zinc extraction (77.1 % to 83.1 %) compared with 100 g/L solids, however, no significant effect was detected for nickel, copper, and iron extractions at 90 °C. Lower solid–liquid ratio resulted in slightly faster leaching kinetics, however, the highest nickel, cobalt, and iron extractions were achieved at 30——60 min with both 50 g/L and 100 g/L solid–liquid ratios, Fig. 2S.

Leaching was also studied in varying acidities ($[H_2SO_4]$ = 0.2 M and 1 M) with 50 g/L solid–liquid ratio. The lower concentration and thus even lower availability of H^+ ions for reactions clearly decreased Ni and Fe dissolution kinetics, whereas the impact on cobalt dissolution was less, Fig. 3. For copper the early leaching kinetics were actually faster at lower acidity, but the final extractions after 6 h did not depend on the acidity. Additionally, copper was shown to precipitate after 2 h leaching at 0.2 M after which the extraction increased again. This behavior can be explained by small fluctuations in pH (0.7–1.0) due to acid consumption and acid additions. Zinc extraction rate and final extraction from sphalerite clearly decreased at lower acidity, which is supported by Reaction 9, Table 1.

Acid consumption (g H_2SO_4 / g Co, Ni, Cu, Zn extracted) was shown to decrease from 86.4 g/g to 63.8 g/g as the leaching acidity was decreased from 1.0 M to 0.2 M H_2SO_4, Fig. 3S (a). The results indicate that high acidity has direct impact on the pyrrhotite and sphalerite dissolution kinetics, potentially supporting chemical leaching of these minerals in the presence of excess acid (Table 1, Reactions 4, 5 and 9). Although, the regeneration of ferrous ions to ferric ions consumes acid according to Reaction 1, previous studies have shown that excess acid can inhibit the regeneration process (Kobe and Dickey, 1945; Iwai et al., 1982). Therefore, at low acidity (0.2 M), the proportion of oxidative reaction pathway may increase (Table 1, Reactions 6 and 10) when compared to the higher acidity (1.0 M).

The final iron extraction in more concentrated sulfuric acid (1 M) was 37.7 % within 15 min whereas at lower acid concentration (0.2 M), in 6 h 30.3 % iron extraction with an increasing trend was found, Fig. 3 (c). This behavior can potentially be explained by continuous oxygen sparging and low oxygen solubility in solution (Gubbins and Walker, 1965), which enables regeneration of dissolved divalent iron species into trivalent, supporting oxidative leaching as a function of time, though with slow kinetics. At higher acidity (1.0 M), the extraction of iron from pyrrhotite was supposedly occurring directly via sulfuric acid only, thus being independent of ferrous/ferric balance. The extraction trends of Fe and Ni suggest that similar final extraction levels can be achieved with both 0.2 and 1.0 M acid if leaching time is extended above 6 h, Fig. 3.

In the previous studies, the leaching of sulfides has been reported to be efficient at relatively low acidities and high oxidation potential. In bio-acid leaching, high Co (59–98 %), Ni (71–98 %), Cu (22–55 %), and Zn (86–98 %) extractions have been achieved from pyrite-pyrrhotite tailings at constant pH = 1.2–1.8 and long leaching times (>7 days) (Mäkinen et al., 2021; Ahmadi et al., 2015; Altinkaya et al., 2018). Xie et al. (2005) showed that doubling sulfuric acid concentration (from 0.05 mL H_2SO_4 / g tailings to 0.1 mL H_2SO_4 / g tailings) slightly increased Co (from 49 % to 51 %) and Ni (from 88 % to 91 %)

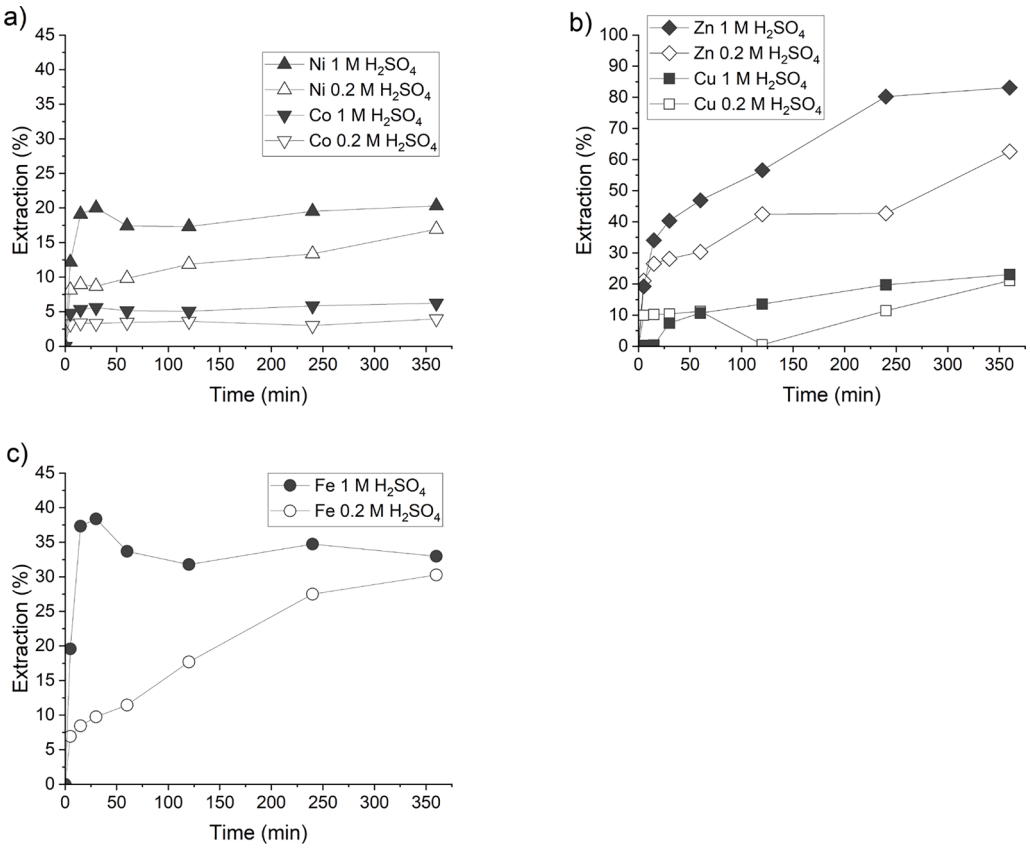

Fig. 3. The effect of sulfuric acid concentration on a) cobalt and nickel, b) zinc and copper and c) iron extraction (Exp. *LA2* and *LA6*: $T = 90$ °C; *S/L-ratio* = 50 g/L; *O_2-flow* = 2 L/min).

extractions from sulfide tailings in sulfuric-nitric acid leaching. However, the study by Xie et al. (2005) concluded that oxidative effect of nitric acid was more significant on metal extractions. Based on the reported results and the results of the current study, increasing acidity can change the leaching mechanism and improve extractions by impacting the kinetics of easily soluble sulfide species such as pyrrhotite and sphalerite. However, for the extraction of refractory sulfide species (pyrite, chalcopyrite etc.) increase in acidity solely does not have an important role, but rather the oxidative leaching mechanism—with strong oxidant—is a necessity.

The effect of oxygen feed (0–2 L/min) was studied at mid-point conditions (T = 60 °C, *S/L-ratio* = 75 g/L, *[H_2SO_4]* = 0.6 M; Exp. *LA10*, *LA12*, *LA15*). In the absence of oxygen feed, it was found that only small extractions of Ni (7.4 %), Co (3.0 %), Zn (24.4 %), Cu (4.7 %), and Fe (4.8 %) were achieved during the first 30 min after which the extractions did not progress any further. With 1 and 2 L/min oxygen feeds and the same conditions, the leaching of metals had slow kinetics, however, metal extractions were increasing until the end of the experiments (at 6 h). The determination of acid consumption during leaching showed that more sulfuric acid was consumed in the absence of oxygen (*LA12*: 171.6 g H_2SO_4 / g Co, Ni, Cu, Zn extracted) than with 1 L/min oxygen feed (*LA15*: 111.7 g H_2SO_4 / g Co, Ni, Cu, Zn extracted) or 2 L/min oxygen feed (*LA10*: 63.9 g H_2SO_4 / g Co, Ni, Cu, Zn extracted) (Fig. 3S (b)). In the presence of oxygen feed, acid dissolution via acid plays a smaller role, whereas the role of ferric leaching appears to be increased.

PLS compositions in H_2SO_4-O_2 leaching experiments are presented in Table 5. Iron extraction was significant (<33.9 %), and through the regeneration of ferric ions by dissolved oxygen, the extracted iron contributed to further metals extractions from the raw material. It has been shown that even minor concentrations of ferric can have a positive effect on the oxidative leaching of sulfide minerals (Hirato et al., 1987; Asadi et al., 2017). The leaching order of minerals follows that reported by Arpalahti and Lundström (2018) as pyrrhotite dissolves before sphalerite, and chalcopyrite is only partially dissolved. From the analyzed elements, zinc was most efficiently extracted, and it has been reported that atmospheric sulfuric acid leaching of sphalerite is an efficient zinc leaching method and ZnS can react via Reactions 9 or 10, Table 1 (Svens et al., 2003). Concentrations of nickel and cobalt in PLS were lower than in industrial Ni-Co solutions (Table 2). However, the achieved nickel concentrations are comparable to nickel concentrations of high-Co solutions from where the nickel—that reports to the raffinate after cobalt solvent extraction—can be potentially further utilized in nickel production (Sole et al., 2005).

Table 5
Metal concentrations of pregnant leach solutions and metal extractions achieved by H_2SO_4-O_2 leaching (*LA1–LA15*).

	Concentration (g/L)	Extraction (%)
Ni	0.016–0.125	3.5–20.3
Co	0.006–0.054	2.3–6.3
Cu	0.004–0.066	1.5–23.4
Zn	0.069–0.618	19.9–78.2
Fe	0.85–17.6	4.0–33.9

SEM-EDS analysis supported the above-mentioned findings as the leach residue from experiment *LA8* contained some cobalt and nickel-containing pyrite, Fig. 4. Additionally, feldspar minerals such as microcline and an albite-ordered mineral were detected.

3.2. Leaching with ferric as oxidant (H_2SO_4-Fe^{3+}–O_2 system)

The effect of ferric iron (*[Fe^{3+}]* = 0.05–0.3 M) as supplementary oxidant was studied in varying sulfuric acid concentrations (*[H_2SO_4]* =

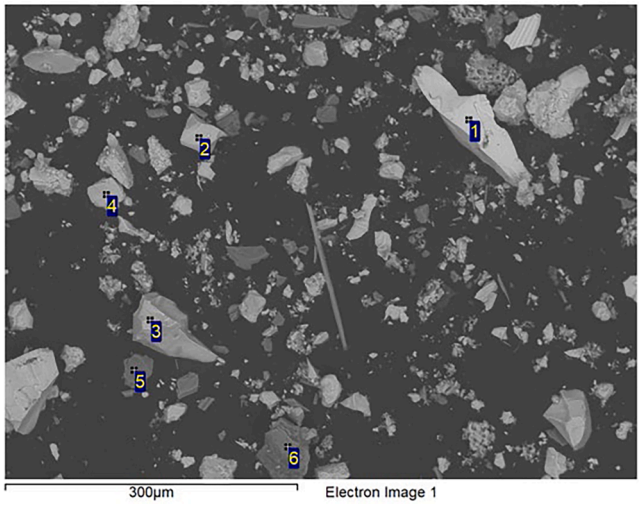

Fig. 4. SEM image of dried leach residue (*LA8*): 1) Co and Ni containing pyrite; 2), 3), and 4) pyrite; 5) albite-ordered mineral and 6) microcline.

0.5–1.0 M) with constant temperature (90 °C), oxygen feed (1 L/min), and solid–liquid ratio (50 g/L) (experiments *LB1-LB8*). The purpose of oxygen feed in leaching series *LB* was to regenerate reduced ferrous ions back to the ferric form. Additionally, the tailings itself releases iron (up to 17.6 g/L with 100 g/L solid–liquid ratio, Table 5) to the leach solution as the leaching proceeds.

By increasing the starting ferric concentration from 0.05 M to 0.3 M, cobalt extraction was increased from 4.8 % to 9.0 % (Fig. 5 (a)) and specifically Fe^{3+} concentrations > 0.1 M had a greater impact on Co extraction. This further confirmed that the main mineral—in which Co is present—was refractory and benefited from higher oxidative power i.e., more oxidant (Fe^{3+}) in the solution. Additionally, the H_2SO_4-Fe^{3+}–O_2 leaching improved zinc and copper extraction rates and final extractions (from 83.1 % to 90.6 % Zn and from 23.1 % to 24.9 % Cu) when compared to the H_2SO_4-O_2 leaching, Fig. 5 (c) and (d).

Similar to the H_2SO_4-O_2 system, copper dissolution was shown to be unstable at lower ferric concentrations ($[Fe^{3+}] < 0.2$ M) due to reprecipitation. Precipitation of copper indicates the presence of H_2S in the leaching solution (Reaction 13, Lu et al., 2023). CuS precipitation by H_2S takes place in wider pH range than sulfide precipitation of nickel, cobalt, and zinc (Monhemius, 1977). As the supplementary ferric concentration increases from 0 to 0.1 M, the precipitation of Cu is delayed which indicates that Cu remains dissolved as long as sufficient ferric concentration is present. From this perspective, these results indicate that the regeneration of ferrous to ferric occurs at slower rate when compared to ferric ion consumption and reduction back to ferrous. Redissolution of precipitated Cu is expected to occur as soon as ferrous ions have sufficiently been regenerated to ferric form. Nevertheless, a more detailed examination of Fe^{2+}/Fe^{3+} balance should be undertaken to confirm the underlying mechanism of Cu extraction and precipitation behavior. From the results it seems that $[Fe^{3+}] = 0.2$ M yields enough oxidative power to solution to avoid Cu precipitation. In general, $[Fe^{3+}] = 0.2$ M was found to provide sufficient ferric concentration for improving cobalt, zinc and copper extractions and leaching kinetics whereas an increase to $[Fe^{3+}] = 0.3$ M had no further positive effect on the leaching behavior of the metals.

$$Cu^{2+} + H_2S \rightarrow CuS + 2H^+ \quad (13)$$

Nickel dissolution was not advanced with increase in ferric concentration. In the leaching series *LB*, the addition of ferric ions to the system was shown to decrease the reaction rate of Ni dissolution (Fig. 5 (b)). However, the final Ni extractions were all in the range of ca. 17.8–20.3 %. Similarities in leaching behaviors of nickel and iron indicate that

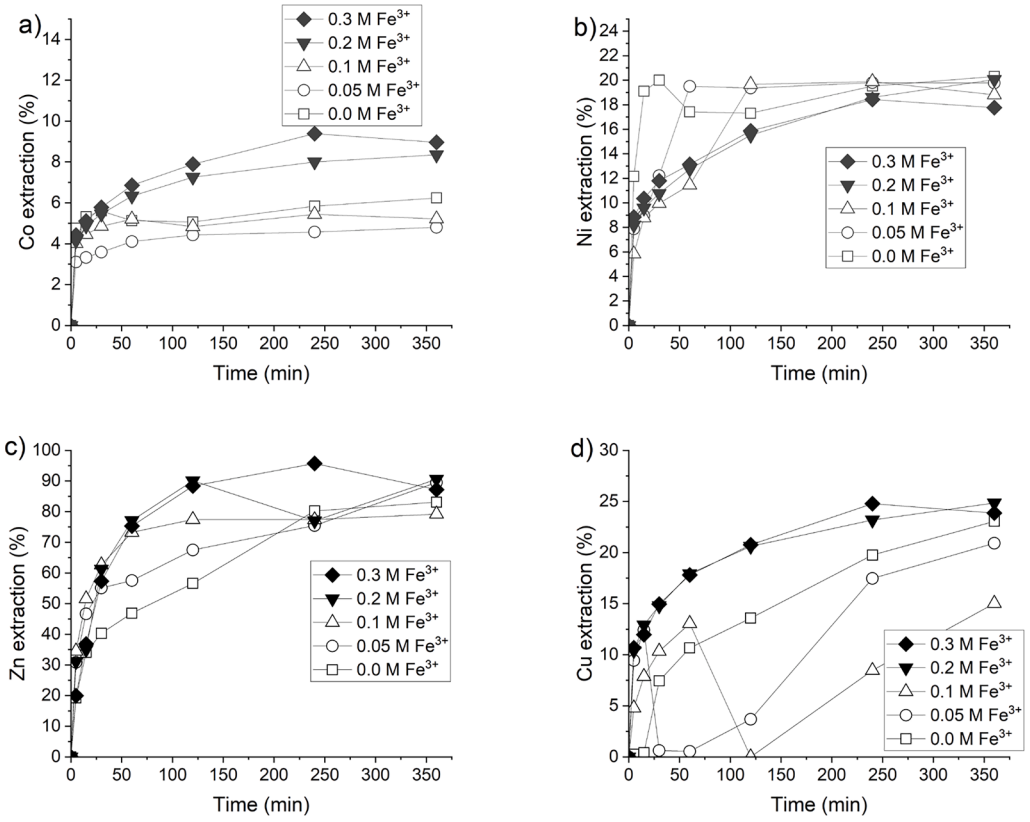

Fig. 5. The effect of added ferric concentration on a) cobalt, b) nickel, c) zinc, and d) copper extraction (Exp. *LA6*, *LB2*, *LB4*, *LB6*, and *LB8*: $T = 90$ °C; *S/L-ratio* = 50 g/L; $[H_2SO_4] = 1$ M).

ferric ions have negative impact on dissolution of Ni-rich pentlandite and pyrrhotite minerals, Fig. 5 (b) and Fig. 6. In the absence of supplementary ferric ions, leaching kinetics of iron are significantly faster, however, the addition of ferric ions contributes to higher redox potential and faster dissolution rate of iron at later stages of leaching. For example, in the absence of initial ferric ions, iron extraction reached 37.3 % within 15 min, whereas in the presence of ferric ions ($[Fe^{3+}]$ = 0.3 M), only 1.9 % of iron is extracted within 15 min but 44.2 % is extracted after 4 h leaching. The results are in line with the ones reported by Garg et al. (2017) who found that the addition of ferric ions results in the formation of elemental sulfur layer around unreacted pyrrhotite particles thus slowing the leaching kinetics of pyrrhotite and decreasing the extraction rates of Ni and Fe. In the presence of dissolved ferric ions and hydrogen sulfide, the precipitation of elemental sulfur occurs via Reaction 14 (Garg et al., 2017). Based on the quantitative XRD analysis of the raw material, the proportions of iron in pyrrhotite, pentlandite, and chalcopyrite were 38.0 %, 0.4 %, and 0.2 %, respectively. As the extraction percentage of iron (44.2 %) clearly exceeds the proportion of iron in the pyrrhotite (38.0 %), the results suggest partial dissolution of pyrite with $[Fe^{3+}]$ = 0.3 M.

$$H_2S + 2Fe^{3+} \rightarrow 2Fe^{2+} + S + 2H^+ \quad (14)$$

The redox potential of the H_2SO_4-Fe^{3+}–O_2 system was generally higher (670–730 mV vs. 190–690 mV (vs. SHE)) in comparison to the H_2SO_4-O_2 system at the beginning of leaching experiments. However, with initial $[Fe^{3+}]$ = 0.2 M (*LB6*), the redox potential decreased from 710 mV to 590 mV (vs. SHE) during 6 h leaching, whereas in the absence of ferric ions (*LA6*), redox potential was increased from 240 mV to 605 mV (vs. SHE). Oxidation and dissolution of pyrite is known to be favored by high redox potential and temperature. Sun et al. (2015) reported that at 75 °C, pyrite extraction being ca. 20 % at 700 mV, ca. 60 % at 800 mV and ca. 92 % at 900 mV (vs. SHE). Hence, it can be concluded that ferric ions and redox potential of the current leaching system was not enough to enhance pyrite dissolution substantially.

In comparison to H_2SO_4-O_2 system, the presence of supplementary ferric ions was shown to reduce the acid consumption during leaching, indicating that more of leaching took place via ferric oxidation of sulfide species (Table 1, Reactions 3, 6, 8, 10 and 12). Nevertheless, acid was still consumed to the oxidation ferrous ions according to Reaction 1. Fig. 4S shows that acid consumption was decreased from 53.3 to 17.1 g H_2SO_4 / g Co, Ni, Cu, Zn extracted as the initial ferric ion concentration was increased from 0.05 M to 0.3 M.

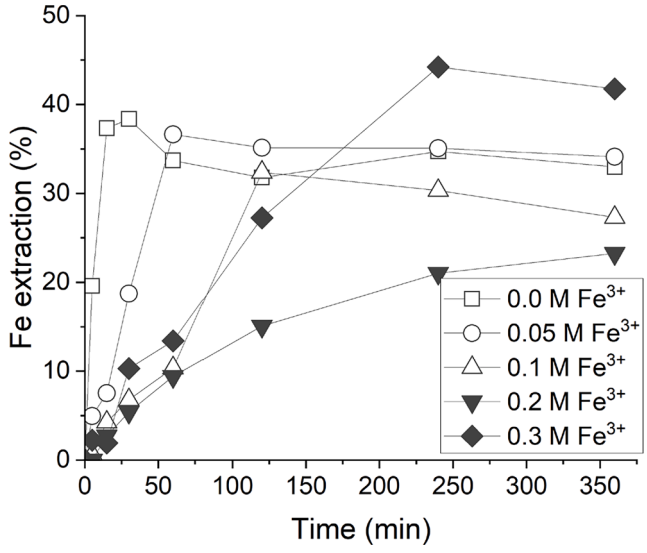

Fig. 6. The effect of added ferric concentration on iron extraction (Exp. *LA6*, *LB2*, *LB4*, *LB6*, and *LB8*: T = 90 °C; *S/L-ratio* = 50 g/L; $[H_2SO_4]$ = 1 M).

Metal concentrations and extractions achieved by H_2SO_4-Fe^{3+}–O_2 leaching are listed in Table 6. In comparison to H_2SO_4-O_2 leaching (Table 5), the high-end concentrations are lower due to lower solid–liquid ratios (50 g/L) in H_2SO_4-Fe^{3+}–O_2 leaching than used in a few of the sulfuric acid leaching experiments (100 g/L). High iron concentrations are contributed by supplementary ferric ions. The addition of ferric ions benefited cobalt, copper, and zinc extractions the most. A beneficial effect of increasing ferric concentration (up to 0.1 M) on chalcopyrite leaching has been reported by Hirato et al. (1987). Santos et al. (2010) showed that only minor improvement can be made in chalcopyrite leaching by increasing ferric concentration from 0.25 M to 0.5 M, whereas the zinc extraction from sphalerite increased from 60 % to 95 %, which is line with the results of this research.

3.3. Leaching with hydrogen peroxide (H_2SO_4-H_2O_2-O_2 system)

The effect of hydrogen peroxide as oxidant was studied at varying temperatures (30–90 °C) (*LC1–LC3*). In the H_2SO_4-O_2 system, most nickel and cobalt extractions—presumably from the pyrrhotite phase—took place within first 30 min of leaching. Hence, it was decided to start the feed of hydrogen peroxide after 30 min of leaching with more hydrogen peroxide added at later sampling times. The redox potential was adjusted to 800 mV (vs. SHE) by hydrogen peroxide at every sampling time after 30 min to boost pyrite dissolution. Hydrogen peroxide can act both as an oxidant and a reductant in leaching, since the oxidation state of oxygen in the molecule is −1 (halfway between O_2 (0) and water (-2)). In acidic solutions, hydrogen peroxide can oxidize sulfide minerals (Salas-Martell et al., 2020), and the presence of hydrogen peroxide can result in reactions shown in Table 7. In sulfuric acid-hydrogen peroxide solution, sulfide minerals react with both acid and peroxide. If the reaction occurs primarily via hydrogen peroxide, sulfide sulfur is oxidized to sulfate according to Reactions 15, 18, and 20. In highly acidic media, pyrite is oxidized by Reaction 16 (Antonijević et al., 1997). At lower anodic potentials and high temperature, reaction occurs primarily via sulfuric acid and sulfide sulfur is oxidized to elemental sulfur according to Reactions 17, 19, and 21.

At 30 °C, both cobalt (3.8 % to 5.3 %) and nickel (6.6 % to 9.6 %) extractions were improved slightly in the presence of hydrogen peroxide (0.5 M) in comparison to H_2SO_4-O_2 leaching. Increase in temperature to 60 °C resulted in 7.0 % and 15.7 % extractions for cobalt and nickel, respectively. At 60 °C, more hydrogen peroxide was required (0.7 M) to maintain redox potential at the desired level. Further increase in temperature to 90 °C and the concentration of hydrogen peroxide (0.8 M) improved cobalt and nickel extractions to 14.2 % and 22.9 %, respectively. Fig. 7 shows the comparison between metals extractions in H_2SO_4-O_2 and H_2SO_4-H_2O_2-O_2 systems at 90 °C. The cobalt extraction was the highest of all applied leaching conditions and the cobalt dissolution proceeded the whole 6 h, suggesting that the pyrite structure started oxidizing and dissolving according to Reactions 15 and 16. As the hydrogen peroxide is consumed, redox potential decreases which favors—along with high temperature—the elemental sulfur formation instead of sulfate and bisulfate according to Reaction 17 (Antonijević et al., 1997). Additionally, the iron extraction (42.0 %) was also higher than in the H_2SO_4-O_2 leaching, supporting the hypothesis of partial

Table 6
Metal concentrations of pregnant leach solutions and metal extractions achieved by H_2SO_4-Fe^{3+}–O_2 leaching (*LB1–LB8*). Fe concentration (g/L) includes both the extracted Fe and added Fe(III) ions, but Fe extraction (%) considers only Fe extracted from the raw material.

	Concentration (g/L)	Extraction (%)
Ni	0.041–0.067	14.1–20.1
Co	0.024–0.059	4.5–9.0
Cu	0.028–0.044	19.8–29.9
Zn	0.302–0.423	79.2–94.2
Fe	10.7–29.4	23.2–41.8

Table 7
Possible leaching reactions (Reactions 15–21) of raw material minerals in sulfuric acid/hydrogen peroxide solution.

Mineral	Reactions	Eq.	Ref.
Pyrite	$2FeS_2 + 15H_2O_2 \rightarrow 2Fe^{3+} + 2SO_4^{2-} + 2H^+ + 14H_2O$	(15)	Salas-Martell et al., 2020
	$2FeS_2 + 15H_2O_2 + 2H^+ \rightarrow 2Fe^{3+} + 4HSO_4^- + 14H_2O$	(16)	
	$2FeS_2 + 3H_2O_2 + 6H^+ \rightarrow 2Fe^{3+} + 4S + 6H_2O$	(17)	
Chalcopyrite	$2CuFeS_2 + 17H_2O_2 + 2H^+ \rightarrow 2Cu^{2+} + 2Fe^{3+} + 4SO_4^{2-} + 18H_2O$	(18)	Antonijević et al., 2004; Sokić et al., 2019
	$2CuFeS_2 + 5H_2O_2 + 10H^+ \rightarrow 2Cu^{2+} + 2Fe^{3+} + 4S + 10H_2O$	(19)	
Sphalerite	$2ZnS + 4H_2O_2 + 2H^+ \rightarrow 2Zn^{2+} + SO_4^{2-} + H_2S + 4H_2O$	(20)	Aydogan, 2006; Pecina et al., 2008
	$ZnS + H_2O_2 + 2H^+ \rightarrow Zn^{2+} + S + 2H_2O$	(21)	

pyrite dissolution.

Addition of hydrogen peroxide accelerated the leaching kinetics of sphalerite as 92.1 % Zn was extracted after 2 h whereas the corresponding extraction in the absence of hydrogen peroxide was 56.6 % which indicates that leaching can be represented by Reactions 20 and 21 in the presence of H_2O_2. Copper extraction was also improved slightly by hydrogen peroxide (23.1 % vs. 30.6 %) and the extraction still had an increasing trend at 6 h (Reactions 18 and 19).

Decrease in redox potential was notable, for example at 90 °C, from 800 to 670–700 mV (vs. SHE) between H_2O_2 additions. The main issue with usage of hydrogen peroxide, as an oxidant, was its decomposition in the presence of dissolved ferric ions (Marzzacco, 1999). Thus, redox potential decreased steadily after hydrogen peroxide addition, and it only partially contributed to the leaching of the tailings. A similar phenomenon was found by Salas-Martell et al. (2020) for the leaching of pyrite-rich ore. Hydrogen peroxide production has a considerable global warming potential (GWP), varying from 442 to 687 kg CO_2 eq per produced ton of 27.5 % H_2O_2 (Jia et al., 2022). Based on the consumed H_2O_2 volume, the GWP of the needed H_2O_2 production for H_2SO_4-H_2O_2-O_2 leaching at 90 °C is 37–58 g CO_2 eq which equals to 133–206 kg CO_2 eq / kg Co, Ni, Cu, Zn extracted. The efficiency of H_2O_2 has been shown previously for pyrite and chalcopyrite leaching (Antonijević et al., 1997; Olubambi and Potgieter, 2009), but the results herein show that from the standpoint of sustainability, the utilization of H_2O_2 is not required in the presence of a sufficient concentration of ferric ions. On the other hand, oxidation reactions by hydrogen peroxide do not further complicate PLS composition which is favorable for metals recovery from the solution.

Table 8 shows the metal concentrations and extractions achieved by H_2SO_4-H_2O_2-O_2 leaching. Cobalt benefited the most from hydrogen peroxide when compared to other studied oxidants (O_2 and Fe^{3+}). In combination with slightly higher nickel and iron extractions, this indicated that the increased metal extractions originate from partially dissolved pyrite that was not dissolved in the presence of O_2 and [Fe^{3+}] <

Table 8
Metal concentrations of pregnant leach solutions and metal extractions achieved by H_2SO_4-H_2O_2-O_2 leaching (*LC1-LC3*).

	Concentration (g/L)	Extraction (%)
Ni	0.021–0.064	8.4–22.9
Co	0.023–0.070	5.2–14.2
Cu	0.018–0.038	16.5–30.8
Zn	0.133–0.323	41.9–89.7
Fe	1.53–9.44	7.7–42.0

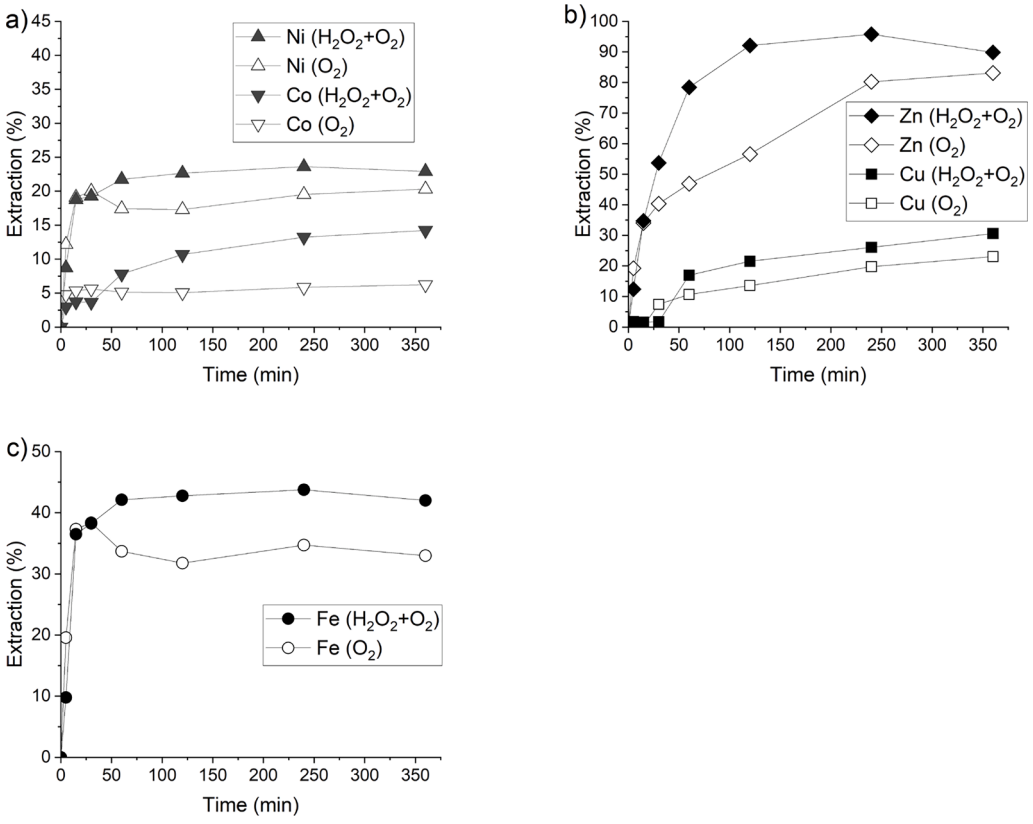

Fig. 7. The effect of hydrogen peroxide on a) nickel and cobalt, b) zinc and copper, and c) iron extraction (Exp. *LA6* and *LC3*: $T = 90$ °C; *S/L-ratio* = 50 g/L; *[H_2SO_4]* = 1 M).

0.3 M. Copper and zinc extractions were in line with the results achieved by H_2SO_4-Fe^{3+}–O_2 leaching.

3.4. Discussion

3.4.1. Tailings and its leaching mechanism

The sulfide tailings used in this study contained pyrite, pyrrhotite, and quartz as main minerals. Additionally, minor minerals included pentlandite, chalcopyrite, and sphalerite. Iron in the raw material was mostly distributed to pyrite and pyrrhotite of which pyrrhotite was effectively totally dissolved during leaching. Nickel is present in pentlandite, but presumably also in pyrrhotite and pyrite. The leaching behavior of nickel resembled that of iron, which indicated that soluble nickel originates from nickeliferous pyrrhotite. The leaching behavior of cobalt suggested that it is mostly present in refractory pyrite and pentlandite, and only a minor fraction (~5%) is present in more soluble minerals such as pyrrhotite. According to mineralogical and elemental analysis, most of the copper is located in chalcopyrite. The sphalerite content of the raw material was not reliably quantified but leaching behavior of zinc indicated that practically all the zinc is found in sphalerite.

In the H_2SO_4-O_2 leaching system, the sulfuric acid concentration (0.2–1 M) and oxygen flow (0–2 L/min) were varied to investigate acid consumption of the leaching and hence, possible changes in leaching mechanism. It was found that oxygen sparging and lower acidity decreased acid consumption / metals extracted i.e., more leaching occurred via oxidative dissolution. However, the leaching kinetics were much faster at higher acidity due to enhanced pyrrhotite extraction. At lower acidity, leaching of Ni, Cu, Zn, and Fe progressed the whole leaching duration (6 h), but final extractions remained below the corresponding extractions at higher acidity. Apparently, the same minerals were dissolving both at lower and higher acidity but with different mechanism. As more acid was consumed / metals extracted at higher acidity (1.0 M), it appears that acid was first consumed directly for the extraction of the pyrrhotite and then for the oxidation of the dissolved ferrous ions. At lower acidity (0.2 M), acid was consumed more for the oxidation of ferrous ions, where the formed ferric ions contributed to the further extraction of pyrrhotite.

Similar behavior was found with H_2SO_4-Fe^{3+}–O_2 leaching; acid consumption decreased further, consistent with the leaching mechanism being preferentially by oxidative dissolution. The positive effect of ferric ions was clearly seen from the early leaching kinetics of Co, Cu, and Zn, however, the effect on the final extractions was moderate. The formation of the sulfur layer around the unreacted pyrrhotite was possibly inhibiting pyrrhotite extraction. A slight improvement can be seen in cobalt extraction which might indicate partial dissolution of more refractory minerals such as pentlandite or pyrite.

Overall, the leaching of pyrrhotite and sphalerite was effective in the studied leaching conditions which is also supported by the literature regarding leaching order of different sulfide species (Arpalahti and Lundström, 2018). From more refractory minerals, chalcopyrite showed slow leaching kinetics, and the extraction of copper could potentially be enhanced by increasing leaching duration. Pyrite is the most refractory mineral of the studied raw material, and the oxidative effect of O_2 and Fe^{3+} was not sufficient for substantial pyrite dissolution. By addition of H_2O_2, pyrite was presumably partially dissolved, however, the H_2O_2 consumption was increased due to decomposition of H_2O_2. Self-decomposition of H_2O_2 can occur by catalysts such as dissolved ferric ions or thermally which can be the case with experiments at 60 °C and 90 °C.

Longer leaching duration or more intensive leaching conditions are necessary for pyrite dissolution meaning either higher temperature and oxygen pressure, i.e., autoclave leaching (Long and Dixon, 2004), roast-leaching (Kamariah et al., 2022), bioleaching (Ahmadi et al., 2015; Altinkaya et al., 2018; Mäkinen et al., 2021), chloride leaching (Altinkaya et al., 2018), intensive milling as pre-treatment (Mäkinen et al., 2021) or use of more oxidizing—but industrially less attractive—chemicals such as HNO_3 (Xie et al., 2005; Teimouri et al., 2022). As drawbacks, these all are likely to increase the capital expenditure and/or operational costs of the leaching process and e.g. nitrates may complicate the solution composition considering integration of the Ni-Co solution into primary solution purification processing.

3.4.2. Suggested processing scenarios

By atmospheric sulfuric acid leaching, pregnant leach solution with low nickel (≈0.1 g/L) and cobalt (≈0.05 g/L) concentrations can be obtained. Additionally, a minor concentration of copper (≈0.05 g/L) and reasonable concentration of zinc (≈0.5 g/L) is present with significant iron impurity concentration (≈15 g/L). In order to utilize the PLS further, Fe must first be removed from the solution. Jarosite and goethite precipitation are the most common methods for iron removal at atmospheric pressure (Chang et al., 2010). Precipitation as jarosite occurs at temperature close to boiling point in the presence of different monovalent cations such as K^+, NH_4^+, and Na^+ (Hoeber and Steinlechner, 2021). Goethite precipitation is generally carried out at pH 2.0–6.0 and at temperature range of 85–95 °C (Chang et al., 2010; Yue et al., 2016). Goethite precipitation does not require added cations and the precipitate is considered more stable for storage than jarosite (Chang et al., 2010). The filtration of the goethite precipitate is generally challenging, and to offset poor filterability, the use of magnetic seed has been proposed (Han et al., 2015).

Following iron removal, pregnant leach solution can potentially be integrated into primary process of nickel–cobalt sulfate solutions prior to solvent extraction stages. The main challenge in integration are the lower metal concentrations when compared to primary nickel–cobalt sulfate solutions (Table 2). In general, primary feed solutions to solvent extraction processes have > 3 g/L Ni or Co depending on the main product and > 0.03 g/L Ni or Co as by-product/impurity. Therefore, the feed ratio of low concentrated Ni-Co solution would have to be low to maintain sufficient metal concentrations in the solvent extraction feed.

An alternative strategy for metals recovery is the precipitation of base metals as intermediate sulfides or hydroxides. Sulfide precipitation can be conducted by means of gaseous hydrogen sulfide (H_2S) or aqueous sodium sulfide (Na_2S), sodium hydrosulfide (NaHS), and ammonium sulfide ($(NH_4)_2S$) of which H_2S is typically utilized at industrial scale. Additionally, solid compounds such as iron sulfide (FeS) and calcium sulfide (CaS) can be used as sulfide sources in precipitation (Lewis, 2010). Iron sulfide has higher solubility than Ni, Co, Zn, and Cu sulfides which enables selective precipitation of these metals with respect to Fe (Zhang and Cheng, 2007). The mixed metal sulfide precipitate can be either subjected to a pyrometallurgical process or redissolved and utilized in primary Ni-Co hydrometallurgical process.

Due to the limited cobalt and nickel extractions from the raw material, the metals were slightly enriched in leach residue when compared to concentrations in the raw material. This especially applies for cobalt; based on the leaching results, the grade of cobalt increased by 50 %—from 0.80 wt% to 1.2 wt%—in H_2SO_4-O_2 leaching (Exp. *LA6*) due to efficient extraction of low cobalt-containing pyrrhotite. Additionally, the nickel grade increased from 0.45 wt% to 0.58 wt% and copper from 0.20 wt% to 0.25 wt%. Therefore, the resulting leach residue can potentially be utilized as a raw material in the primary nickel–cobalt sulfide smelting process. In general, sulfide processes including mines, concentrators, and smelting are considered profitable when Ni, Co, and Cu concentrations are greater than 2 wt% in combination (Crundwell et al., 2011). Fig. 8 summarizes different processing strategies for Ni-Co sulfate solution and Ni-Co sulfide residue.

4. Conclusions

The aim of this research was to study the possibility of extracting valuable battery metals from flotation tailings using atmospheric leaching conditions. Additionally, the target was to extract the metals in

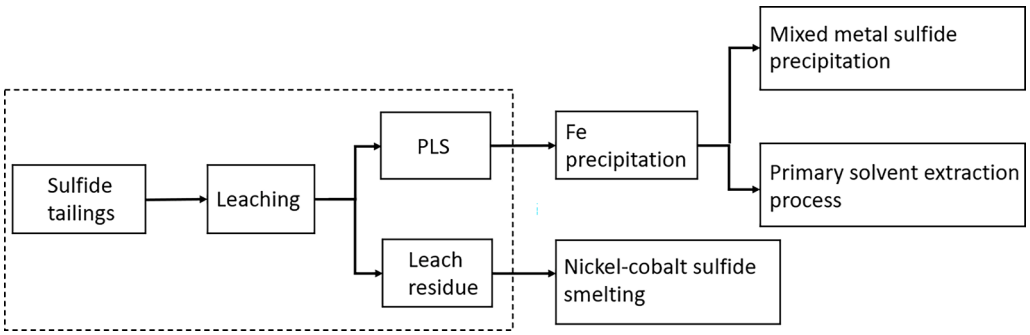

Fig. 8. Potential processing strategies for sulfide tailings via pregnant leach solution (PLS) and leach residue valorization. Dashed lines represent the scope of the experimental work in this study.

a way that the pregnant leach solution would have suitable characteristics for integration into primary battery metals production. Therefore, the leaching was carried out in sulfate media and in the presence of oxidants that wouldn't complicate the pregnant leach solution further.

For cobalt extraction from the tailings, the most oxidative conditions are beneficial. The final Co extraction was ca. 6 % in the H_2SO_4-O_2 system, ca. 9 % in the H_2SO_4-Fe^{3+}–O_2 system and ca. 14 % in H_2SO_4-H_2O_2-O_2 system which indicated that partial pyrite dissolution took place at elevated oxidation potentials. Based on the similar leaching trends between nickel and iron, the extracted nickel was mainly present in pyrrhotite. Pyrrhotite leaching was complete in the H_2SO_4-O_2 system, which explains the moderate increase in Ni extraction in more oxidative conditions—from ca. 20 % to 23 %. Copper extraction increased the whole leaching duration which shows the slow leaching kinetics of chalcopyrite. Zinc extraction from sphalerite was shown to be efficient during atmospheric sulfuric acid leaching which is also supported by the literature. The use of oxidants seemingly reduced the acid dissolution of minerals and increased the oxidative dissolution, however, the change in leaching mechanism had only a small effect on the final metal extractions.

To enhance metals extraction from the tailings or other pyrite-rich materials, a longer leaching time or more intensive conditions are needed. On the other hand, atmospheric sulfuric acid leaching is an efficient method for cobalt and nickel extraction from non-refractory minerals such as pyrrhotite as well as for zinc extraction from sphalerite. Therefore, the leaching approach presented in this research shows potential for the treatment of high-pyrrhotite tailings.

CRediT authorship contribution statement

Anssi Karppinen: Conceptualization, Methodology, Validation, Investigation, Writing – original draft. **Sipi Seisko:** Conceptualization, Methodology, Writing – review & editing. **Mari Lundström:** Conceptualization, Methodology, Writing – review & editing, Supervision.

Declaration of Competing Interest

The authors declare that they have no known competing financial interests or personal relationships that could have appeared to influence the work reported in this paper.

Data availability

Data will be made available on request.

Acknowledgements

This study was supported by BATCircle2.0 project (grant number 44886/31/2020), financed by Business Finland. The authors have made use of Finland's RawMatTERS Finland Infrastructure (RAMI) based in Aalto University and funded by the Academy of Finland. The authors are grateful to Boliden AB for providing the raw material. Authors would like to thank Pasi Heikkilä (GTK, Finland) for providing assistance related to material characterization.

Appendix A. Supplementary data

Supplementary data to this article can be found online at https://doi.org/10.1016/j.mineng.2024.108576.

References

Abraitis, P.K., Pattrick, R.A.D., Vaughan, D.J., 2004. Variations in the compositional, textural and electrical properties of natural pyrite: a review. Int. J. Miner. Process. 74 (1–4), 41–59. https://doi.org/10.1016/j.minpro.2003.09.002.

Ahmadi, A., Khezri, M., Abdollahzadeh, A.A., Askari, M., 2015. Bioleaching of copper, nickel and cobalt from the low grade sulfidic tailing of Golgohar Iron Mine. Iran. Hydrometallurgy 154, 1–8. https://doi.org/10.1016/j.hydromet.2015.03.006.

Altinkaya, P., Mäkinen, J., Kinnunen, P., Kolehmainen, E., Haapalainen, M., Lundström, M., 2018. Effect of biological pretreatment on metal extraction from flotation tailings for chloride leaching. Miner. Eng. 129, 47–53. https://doi.org/10.1016/j.mineng.2018.09.012.

Antonijević, M.M., Dimitrijević, M., Janković, Z., 1997. Leaching of pyrite with hydrogen peroxide in sulphuric acid. Hydrometall. 46 (1–2), 71–83.

Antonijević, M.M., Janković, Z.D., Dimitrijević, M.D., 2004. Kinetics of chalcopyrite dissolution by hydrogen peroxide in sulphuric acid. Hydrometall. 71 (3–4), 329–334. https://doi.org/10.1016/S0304-386X(03)00082-3.

Arpalahti, A., Lundström, M., 2018. The leaching behavior of minerals from a pyrrhotite-rich pentlandite ore during heap leaching. Miner. Eng. 119, 116–125. https://doi.org/10.1016/j.mineng.2018.01.025.

Asadi, T., Azizi, A., Lee, J.C., Jahani, M., 2017. Leaching of zinc from a lead-zinc flotation tailing sample using ferric sulphate and sulfuric acid media. J. Environ. Chem. Eng. 5 (5), 4769–4775. https://doi.org/10.1016/j.jece.2017.09.005.

Aydogan, S., 2006. Dissolution kinetics of sphalerite with hydrogen peroxide in sulphuric acid medium. Chem. Eng. J. 123 (3), 65–70. https://doi.org/10.1016/j.cej.2006.07.001.

Braun, R.L., Lewis, A.E., Wadsworth, M.E., 1974. In-place leaching of primary sulfide ores: laboratory leaching data and kinetics model. Metallurgical Transactions 5, 1717–1726.

Chang, Y., Zhai, X., Li, B., Fu, Y., 2010. Removal of iron from acidic leach liquor of lateritic nickel ore by goethite precipitate. Hydrometall. 101 (1–2), 84–87. https://doi.org/10.1016/j.hydromet.2009.11.014.

Chirita, P., Preda, M., Rusu, O., 2002. Natural pyrrhotite dissolution in aqueous solution. Southern Brazilian Journal of Chemistry 10 (11), 11–17.

Cole, P.M., 2002. The introduction of solvent-extraction steps during upgrading of a cobalt refinery. Hydrometall. 64 (1), 69–77. https://doi.org/10.1016/S0304-386X(02)00013-0.

Crundwell, F., Moats, M., Ramachandran, V., Robinson, T., Davenport, W.G., 2011. Extractive metallurgy of nickel, cobalt and platinum group metals. Elsevier.

Dehaine, Q., Tijsseling, L.T., Glass, H.J., Törmänen, T., Butcher, A.R., 2021. Geometallurgy of cobalt ores: A review. Miner. Eng. 160, 106656 https://doi.org/10.1016/j.mineng.2020.106656.

Descostes, M., Vitorge, P., Beaucaire, C., 2004. Pyrite dissolution in acidic media. GeochimicaEt Cosmochimica Acta 68 (22), 4559–4569. https://doi.org/10.1016/j.gca.2004.04.012.

Donegan, S., 2006. Direct solvent extraction of nickel at Bulong operations. Miner. Eng. 19 (12), 1234–1245. https://doi.org/10.1016/j.mineng.2006.03.003.

Eksteen, J.J., Oraby, E.A., Nguyen, V., 2020. Leaching and ion exchange based recovery of nickel and cobalt from a low grade, serpentine-rich sulfide ore using an alkaline glycine lixiviant system. Miner. Eng. 145, 106073 https://doi.org/10.1016/j.mineng.2019.106073.

Estay, H., Barros, L., Troncoso, E., 2021. Metal sulfide precipitation: Recent breakthroughs and future outlooks. Minerals 11 (12), 1385. https://doi.org/10.3390/min11121385.

Faraji, F., Alizadeh, A., Rashchi, F., Mostoufi, N., 2022. Kinetics of leaching: A review. Rev. Chem. Eng. 38 (2), 113–148. https://doi.org/10.1515/revce-2019-0073.

Feather, A., Bouwer, W., Swarts, A., Nagel, V., 2002. Pilot-plant solvent extraction of cobalt and nickel for Avmin's Nkomati project. J. South Afr. Inst. Min. Metall. 102 (8), 457–461.

Garg, S., Judd, K., Mahadevan, R., Edwards, E., Papangelakis, V.G., 2017. Leaching characteristics of nickeliferous pyrrhotite tailings from the Sudbury. Ontario Area. Canadian Metallurgical Quarterly 56 (4), 372–381.

Gubbins, K.E., Walker, R.D., 1965. The solubility and diffusivity of oxygen in electrolytic solutions. J. Electrochem. Soc. 112 (5), 469–471.

Han, H., Sun, W., Hu, Y., Tang, H., Yue, T., 2015. Magnetic separation of iron precipitate from nickel sulfate solution by magnetic seeding. Hydrometall. 156, 182–187. https://doi.org/10.1016/j.hydromet.2015.07.001.

Hirato, T., Majima, H., Awakura, Y., 1987. The leaching of chalcopyrite with ferric sulfate. Metallurgical Transactions B 18, 489–496.

Hiroyoshi, N., Arai, M., Miki, H., Tsunekawa, M., Hirajima, T., 2002. A new reaction model for the catalytic effect of silver ions on chalcopyrite leaching in sulfuric acid solutions. Hydrometall. 63 (3), 257–267. https://doi.org/10.1016/S0304-386X(01)00228-6.

Hoeber, L., Steinlechner, S., 2021. A comprehensive review of processing strategies for iron precipitation residues from zinc hydrometallurgy. Cleaner Engineering and Technology 4, 100214. https://doi.org/10.1016/j.clet.2021.100214.

Holmes, P.R., Crundwell, F.K., 2000. The kinetics of the oxidation of pyrite by ferric ions and dissolved oxygen: an electrochemical study. GeochimicaEt Cosmochimica Acta 64 (2), 263–274. https://doi.org/10.1016/S0016-7037(99)00296-3.

IEA (2021), World Energy Outlook 2021, IEA, Paris https://www.iea.org/reports/world-energy-outlook-2021, License: CC BY 4.0.

Iwai, M., Majima, H., Awakura, Y., 1982. Oxidation of Fe (II) in sulfuric acid solutions with dissolved molecular oxygen. Metall. Trans. B 13, 311–318.

Janzen, M.P., Nicholson, R.V., Scharer, J.M., 2000. Pyrrhotite reaction kinetics: reaction rates for oxidation by oxygen, ferric iron, and for nonoxidative dissolution. GeochimicaEt Cosmochimica Acta 64 (9), 1511–1522.

Jia, Y., Bai, Y., Chang, J., Zhai, Y., Zhang, T., Ren, K., Hong, J., 2022. Life cycle assessment of hydrogen peroxide produced from mainstream hydrogen sources in China. J. Clean. Prod. 352, 131655 https://doi.org/10.1016/j.jclepro.2022.131655.

Jorjani, E., Ghahreman, A., 2017. Challenges with elemental sulfur removal during the leaching of copper and zinc sulfides, and from the residues; a review. Hydrometall. 171, 333–343. https://doi.org/10.1016/j.hydromet.2017.06.011.

Kamariah, N., Kalebic, D., Xanthopoulos, P., Blannin, R., Araujo, F.P., Koelewijn, S.F., Spooren, J., 2022. Conventional versus microwave-assisted roasting of sulfidic tailings: Mineralogical transformation and metal leaching behavior. Miner. Eng. 183, 107587 https://doi.org/10.1016/j.mineng.2022.107587.

Kobe, K.A., Dickey, W., 1945. Oxidation of Ferrous Sulfate Solutions with Oxygen. Ind. Eng. Chem. 37 (5), 429–431.

Kursunoglu, S., Ichlas, Z.T., Kaya, M., 2017. Solvent extraction process for the recovery of nickel and cobalt from Caldag laterite leach solution: The first bench scale study. Hydrometall. 169, 135–141. https://doi.org/10.1016/j.hydromet.2017.01.001.

Laidler, K.J., 1984. The development of the Arrhenius equation. J. Chem. Educ. 61 (6), 494–498.

Lewis, A.E., 2010. Review of metal sulphide precipitation. Hydrometall. 104 (2), 222–234. https://doi.org/10.1016/j.hydromet.2010.06.010.

Long, H., Dixon, D.G., 2004. Pressure oxidation of pyrite in sulfuric acid media: a kinetic study. Hydrometall. 73 (3–4), 335–349. https://doi.org/10.1016/j.hydromet.2003.07.010.

Lu, J., Dreisinger, D., 2013. Copper leaching from chalcopyrite concentrate in Cu (II)/Fe (III) chloride system. Miner. Eng. 45, 185–190. https://doi.org/10.1016/j.mineng.2013.03.007.

Lu, Z.Y., Jeffrey, M.I., Zhu, Y., Lawson, F., 2000. Studies of pentlandite leaching in mixed oxygenated acidic chloride-sulfate solutions. Hydrometall. 56 (1), 63–74. https://doi.org/10.1016/S0304-386X(00)00067-0.

Lu, X., Li, Y., Zhang, A., Luo, G., Wu, X., Wang, S., Guo, Y., 2023. Highly efficient and selective removal of copper from low pH nickel Watts solution through hydrogen sulfide. Chem. Pap. 77 (11), 6707–6715. https://doi.org/10.1007/s11696-023-02970-6.

Magwaneng, R.S., Batnasan, A., Haga, K., Shibayama, A., 2017. Development of a Combined Flotation and High Pressure Leaching Process for Copper and Nickel Recovery from Mine Tailing. J. Miner. Mater. Charact. Eng. 5 (03), 118–131. https://doi.org/10.4236/jmmce.2017.53010.

Mäkinen, J., Heikola, T., Salo, M., Kinnunen, P., 2021. The effects of milling and pH on Co, Ni, Zn and Cu bioleaching from polymetallic sulfide concentrate. Minerals 11 (3), 317. https://doi.org/10.3390/min11030317.

Marzzacco, C.J., 1999. The enthalpy of decomposition of hydrogen peroxide: a general chemistry calorimetry experiment. J. Chem. Educ. 76 (11), 1517–1518. https://doi.org/10.1021/ed076p1517.

Michaux, S.P., 2021a. The Mining of Minerals and the Limits to Growth. Geological Survey of Finland: Espoo, Finland. DOI:10.13140/RG.2.2.10175.84640.

Michaux, S.P., 2021b. Assessment of the Extra Capacity Required of Alternative Energy Electrical Power Systems to Completely Replace Fossil Fuels. Geological Survey of Finland: Espoo, Finland. DOI:10.13140/RG.2.2.34895.00160.

Monhemius, A.J., 1977. Precipitation diagrams for metal hydroxides, sulphides, arsenates and phosphates. Transactions of the Institutions of Mining & Metallurgy, Section C 86, 202–206.

Murphy, R., Strongin, D.R., 2009. Surface reactivity of pyrite and related sulfides. Surf. Sci. Rep. 64 (1), 1–45. https://doi.org/10.1016/j.surfrep.2008.09.002.

Nayak, A., Jena, M.S., Mandre, N.R., 2022. Beneficiation of lead-zinc ores–a review. Miner. Process. Extr. Metall. Rev. 43 (5), 564–583. https://doi.org/10.1080/08827508.2021.1903459.

Olubambi, P.A., Potgieter, J.H., 2009. Investigations on the mechanisms of sulfuric acid leaching of chalcopyrite in the presence of hydrogen peroxide. Miner. Process. Extr. Metall. Rev. 30 (4), 327–345. https://doi.org/10.1080/08827500902958191.

Ozer, M., 2019. Cobalt and copper recovery from the ancient flotation tailings by selective sulfation roast-leaching process. J. Min. Metall. Sect. B. 55 (3), 315–324. https://doi.org/10.2298/JMMB1903040430.

Pecina, T., Franco, T., Castillo, P., Orrantia, E., 2008. Leaching of a zinc concentrate in H2SO4 solutions containing H2O2 and complexing agents. Miner. Eng. 21 (1), 23–30. https://doi.org/10.1016/j.mineng.2007.07.006.

Sahu, S.K., Agrawal, A., Pandey, B.D., Kumar, V., 2004. Recovery of copper, nickel and cobalt from the leach liquor of a sulphide concentrate by solvent extraction. Miner. Eng. 17 (7–8), 949–951. https://doi.org/10.1016/j.mineng.2004.03.009.

Salas-Martell, D., Pareja-Guzman, G., Tello-Hijar, J., Rodriguez-Reyes, J.C.F., 2020. Leaching of a pyrite-based ore containing copper using sulfuric acid and hydrogen peroxide. International Journal of Industrial Chemistry 11 (3), 195–201. https://doi.org/10.1007/s40090-020-00212-2.

Samadifard, N., Devine, C.E., Edwards, E., Mahadevan, K., Papangelakis, V.G., 2015. Ferric sulfate leaching of pyrrhotite tailings between 30 to 55 C. Minerals 5 (4), 801–814. https://doi.org/10.3390/min5040526.

Santos, S.M., Machado, R.M., Correia, M.J.N., Reis, M.T.A., Ismael, M.R.C., Carvalho, J. M., 2010. Ferric sulphate/chloride leaching of zinc and minor elements from a sphalerite concentrate. Miner. Eng. 23 (8), 606–615. https://doi.org/10.1016/j.mineng.2010.02.005.

Savinova, E., Evans, C., Lèbre, É., Stringer, M., Azadi, M., Valenta, R.K., 2023. Will global cobalt supply meet demand? The geological, mineral processing, production and geographic risk profile of cobalt. Resour. Conserv. Recycl. 190, 106855 https://doi.org/10.1016/j.resconrec.2022.106855.

Sirkeci, A.A., Gül, A., Bulut, G., Arslan, F., Onal, G., Yuce, A.E., 2006. Recovery of Co, Ni, and Cu from the tailings of divrigi iron ore concentrator. Miner. Process. Extr. Metall. Rev. 27 (2), 131–141. https://doi.org/10.1080/08827500600563343.

Sokić, M., Marković, B., Stanković, S., Kamberović, Ž., Štrbac, N., Manojlović, V., Petronijević, N., 2019. Kinetics of chalcopyrite leaching by hydrogen peroxide in sulfuric acid. Metals 9 (11), 1173. https://doi.org/10.3390/met9111173.

Sole, K.C., Feather, A.M., Cole, P.M., 2005. Solvent extraction in southern Africa: An update of some recent hydrometallurgical developments. Hydrometall. 78 (1–2), 52–78. https://doi.org/10.1016/j.hydromet.2004.11.012.

Sun, H., Chen, M., Zou, L., Shu, R., Ruan, R., 2015. Study of the kinetics of pyrite oxidation under controlled redox potential. Hydrometall. 155, 13–19. https://doi.org/10.1016/j.hydromet.2015.04.003.

Svens, K., Kerstiens, B., Runkel, M., 2003. Recent experiences with modern zinc processing technology. Erzmetall 56 (2), 94–103.

Teimouri, S., Potgieter, J.H., van Dyk, L., Billing, C., 2022. The kinetics of pyrite dissolution in nitric acid solution. Materials 15 (12), 4181. https://doi.org/10.3390/ma15124181.

Xiao, W., Liu, X., Zhao, Z., 2020. Kinetics of nickel leaching from low-nickel matte in sulfuric acid solution under atmospheric pressure. Hydrometall. 194, 105353 https://doi.org/10.1016/j.hydromet.2020.105353.

Xie, Y., Xu, Y., Yan, L., Yang, R., 2005. Recovery of nickel, copper and cobalt from low-grade Ni–Cu sulfide tailings. Hydrometall. 80 (1–2), 54–58. https://doi.org/10.1016/j.hydromet.2005.07.005.

Yue, T., Han, H., Sun, W., Hu, Y., Chen, P., Liu, R., 2016. Low-pH mediated goethite precipitation and nickel loss in nickel hydrometallurgy. Hydrometall. 165, 238–243. https://doi.org/10.1016/j.hydromet.2016.03.004.

Zhang, W., Cheng, C.Y., 2007. Manganese metallurgy review. Part II: Manganese separation and recovery from solution. Hydrometall. 89 (3–4), 160–177. https://doi.org/10.1016/j.hydromet.2007.08.009.